Aeroelastic Limit Cycle Oscillation Analysis of Two Geometrically Identical Wings with Differing Mass Properties

Ethan Sites[1] and Matthew Bryant[2]
North Carolina State University, Raleigh, NC, 27695, USA

An aeroelastic wing placed downstream of a variable frequency disturbance generator can experience limit cycle oscillations (LCOs) under certain conditions. One such condition is when the rate at which the vortices are produced is just below the inherent LCO frequency of the wing. The goal of studying these disturbances is to tailor them to gain a greater understanding of the interaction between aeroelastic systems and incoming flow disturbances. A design update to the aeroelastic wing replaced the existing one to prevent structural faults while maintaining the same airfoil shape, center of mass, and length. The new aeroelastic wing was fabricated using SLA resin 3D printing and sanded and painted multiple times to achieve a smooth surface finish. Changes in the endplate material and main spar diameter also changed the moment of inertia at the center of mass. Both wings were tested in the NCSU subsonic wind tunnel and entered self-sustaining LCO at a dynamic pressure as low as 19.15 Pa without the disturbance generator present, with each wing requiring different initial conditions. To determine the LCO frequency, the wind tunnel speed was increased, and the wing was manually excited by hand, recording the frequency as it entered LCO. To find the relationship between LCO amplitude and wind tunnel speed with and without the disturbance generator placed upstream, the LCO amplitudes were recorded as wind tunnel speed was increased. With the disturbance generator placed upstream, the wings entered LCO at higher wind tunnel speeds. The new wing, with increased mass, offers a new data point in the study of multiple aeroelastic systems. When compared to the existing wing, the increased mass of the new aeroelastic wing showed changes in LCO frequency and root mean square pitch and heave amplitude. This work demonstrates a relationship between mass properties and LCO properties, as well as offering insight into improving characteristics of LCO.

I. Nomenclature

A_{rms}	=	root mean square amplitude of oscillation
f_{peak}	=	peak frequency
f_2	=	second peak frequency
f_3	=	third peak frequency
q	=	dynamic pressure

II. Introduction

The Intelligent Systems and Structures Research Lab (iSSRL) under Dr. Matthew Bryant is conducting a project to examine the effects of flow disturbances caused by a variable frequency disturbance generator placed upstream of an aeroelastic wing. Research has shown that these disturbances modulate and annihilate limit cycle oscillations (LCOs) experienced by the downstream aeroelastic wing [1-3]. Many aeroelastic systems such as aircraft wings are susceptible to LCOs. Some studies have been conducted on the F/A-18C/D with wing-tip missiles on [4-6], which requires an Active Oscillation Control (AOC) system to suppress the LCOs.

The ability to actuate and control these disturbances will lead to greater understanding of the interaction between aeroelastic systems experiencing LCO and incoming flow disturbances. This understanding could not only lead to

[1] Undergraduate, Department of Mechanical and Aerospace Engineering, Student Member AIAA #1179550
[2] Associate Professor, Department of Mechanical and Aerospace Engineering

suppression methods in real-world systems, but also power generation through aeroelastic vibration power harvesting. Bryant and Garcia [7-9] developed and tested an aeroelastic power harvester using piezoelectric materials as smaller alternative to wind turbines. Furthermore, Bryant and Chatterjee [10] have combined piezoelectric benders into a photovoltaic ribbon to show negligible performance penalty in adding wind energy harvesting capability to the solar cells.

The iSSRL previously designed and implemented a 3D printed wing section to examine the aeroelastic properties behind the disturbance generator. During testing, repeated motion caused lateral cracks to develop along the wing surface, which had been patched during testing but continued to appear. If not properly addressed, this could result in unreliable data. The goal of this design update is to replace the existing aeroelastic wing with a new one to prevent these faults from occurring. Design constraints for the new wing were put in place to keep the same airfoil shape, center of mass, and length as the existing wing to match as many physical properties as possible to ensure compatibility with existing research hardware. Towards the end of the project, the old wing was also restored using the same process as the new wing.

The second goal of the design update is to fabricate a new instrumented static wing that experiences vortices while remaining stationary. This design is based on the aeroelastic wing geometry but will include pressure sensors and electronics on the inside. The pressure ports are placed at the center of the wing and in the direction of the wing chord. The pressure sensors allow the real time analysis of the pressure distribution and investigation of the effect of disturbances generated by the upstream bluff body. With the design in place, further work will be done to fabricate and test the wing.

III. Methodology

A. Aeroelastic Wing Design

The aeroelastic wing airfoil is a decambered SD7003 symmetrical airfoil with a span of 600 mm. To strengthen the skin of the wing, the thickness was increased to 2 mm, thereby increasing the mass. Square corners on the interior voids of the wing structure were filleted to increase strength around the spars. While these changes would cause the wing mass to increase and change inertial properties, the center of mass of the new wing was verified in SolidWorks to be the same as the original, 64.9mm behind the leading edge. Initial testing of the wing is used to verify that the new wing can attain LCO and record any differences from the changes in inertia.

The material of the new wing was also changed to Stratasys VeroPureWhite from ABS, seen in the uncoated wing in Figure 1. VeroPureWhite has a modulus of elasticity of 2,495 MPa, higher than ABS with an average modulus of elasticity of 2,050 MPa, making it a better choice to prevent displacement in areas such as the ribs of the wing. A Stratasys Objet30 Printer was used to 3D print the wing section. With a 16-micron resolution, the printer can provide a better surface finish before post-processing. To fit in the Objet30, the wing was divided into three equal-span sections. Two 5/16” Diameter 6061 Aluminum Rods were used as spars for the wing, as well as a 1/16” Diameter 4140 Alloy steel rod for alignment towards the trailing edge.

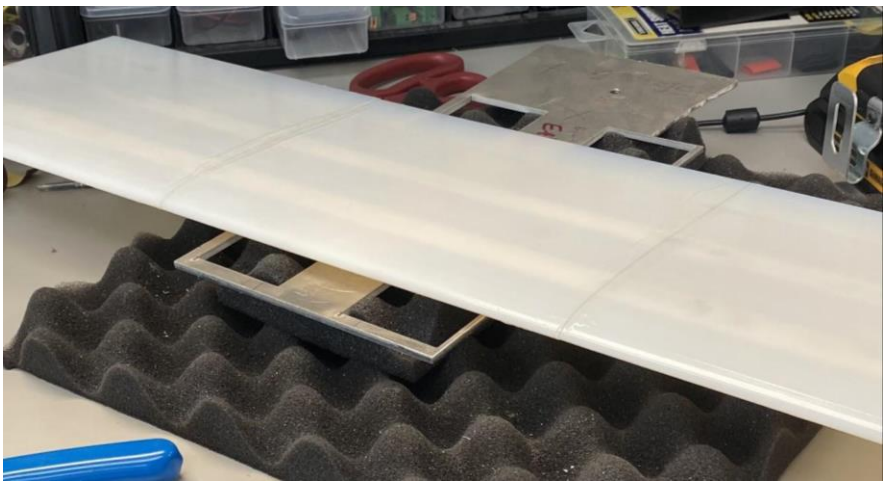

Fig. 1 Aeroelastic wing immediately after printing with 3 sections attached by spar and epoxy.

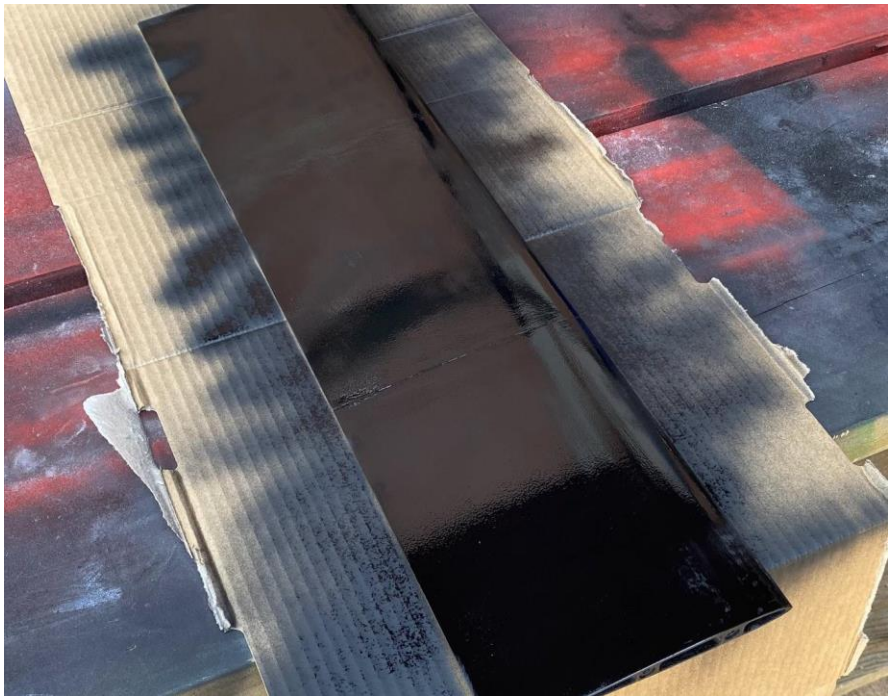

Fig. 2 Aeroelastic wing immediately after spray painting.

The surface of the wing was sanded, painted, and had a clear coat applied to ensure the smoothest finish. The painting process can be seen in Figure 2. As per the method of Visbal and Garman [3], endplates were attached to both sides of the wing to prevent the effects of wingtip vortices and simulate the effects of 2D flow in 3D. The endplates were laser cut from hardboard and had monocoat applied to the surface to cover any holes and form a smooth surface. Aluminum plates, designed in SolidWorks and manufactured by waterjet cutting, were attached outside the hardboard plates and held the whole assembly together.

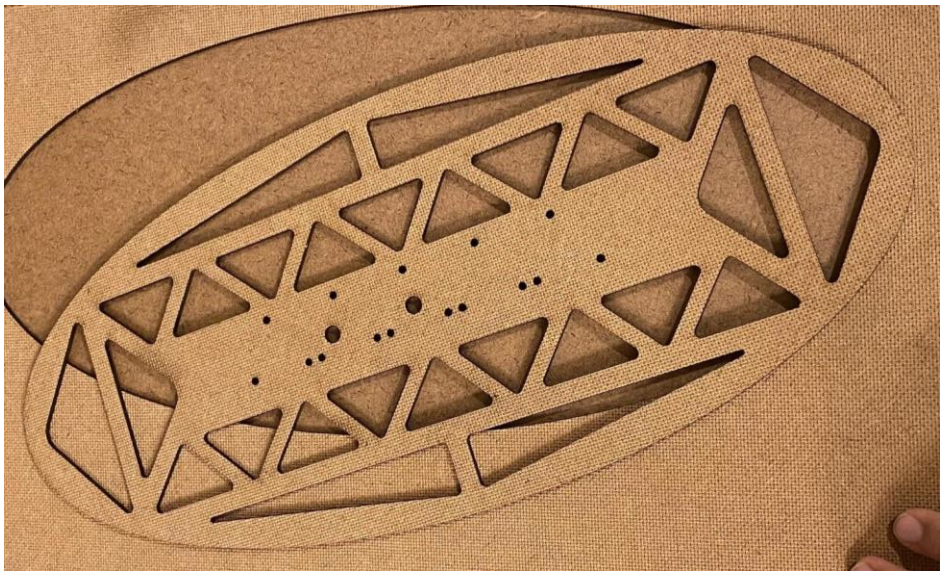

Fig. 3 Endplate for aeroelastic wing after laser cutting.

Fig. 4 Aeroelastic wing fully sanded, painted, and assembled with monocoat on endplates.

With these changes, the mass of the aeroelastic wing increased by 262 grams, from 754 grams to 1016 grams. From the previous assembly by Gianikos et al [1], the total mass and mass of all rotating parts are 3.27 kg and 1.61 kg, and therefore by subtracting the old wing mass and adding the new wing mass gives a new total mass and mass of all rotating parts of 3.532 kg and 1.872 kg. The previous moment of inertia about the center of mass of the old wing assembly was determined using SolidWorks to be 3.897e-03 kg-m^2. By recreating the assembly in SolidWorks and replacing the old wing with the new wing, the new moment of inertia is found to be 4.708e-03 kg-m^2. A summary of the mass properties of both the old and new wings is found in Table 1.

Table 1 Comparison of old and new aeroelastic wing

Property	Old wing	New wing
Wing Material	ABS Plastic	VeroPureWhite
Endplate Material	Birch Ply	Hardboard
Main Spar Diameter	1/8”	5/16”
Wing Mass	0.754 kg	1.016 kg
Mass of all rotating parts	1.61 kg	1.87 kg
Total Mass of all moving parts	3.27 kg	3.532 kg
Center of mass location behind leading edge	64.9 mm	64.9 mm
Moment of inertia taken at the center of mass	3.897e-03 kg-m^2	4.708e-03 kg-m^2

B. Wind Tunnel Testing

Testing of the aeroelastic wing was performed in the NCSU closed-return subsonic wind tunnel with a 0.81 x 1.14 x 1.17 m test section. This experiment's purpose was to validate the design and ensure that the wing response in the presence of the variable frequency disturbance generator is comparable to data from the former wing, as well as determining whether the wing can enter LCO in the same range of flow conditions. First, the disturbance generator, composed of a cylinder and splitter plate, was placed in the wind tunnel at a distance of 8 cylinder-diameters upstream of the wing. Both the disturbance generator and wing use US Digital E6-10000 optical encoders to return pitch angle data, and the wing also has a Renishaw LM10 magnetic linear encoder to return heave data. Data was recorded in LabVIEW with the use of a National Instruments PXIe-1078, with a minimum resolution of 1000 Hz.

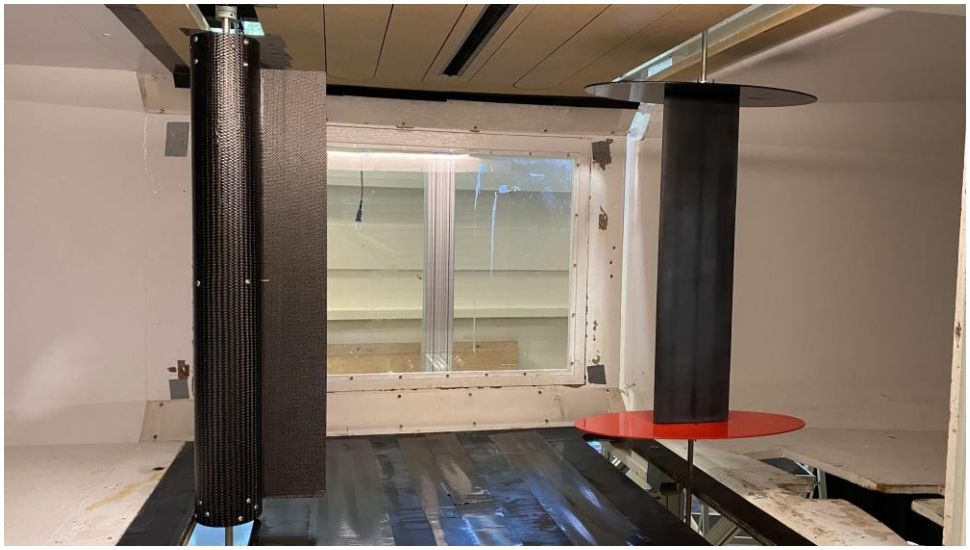

Fig. 5 Wind tunnel test section with disturbance generator (left) and aeroelastic wing (right).

The following experiments were conducted to determine the LCO frequency with and without the upstream disturbance generator. Wind tunnel speed was increased from 23.94 Pa to 47.88 Pa in steps of 4.79 Pa and manual LCO excitation was attempted at every iteration. Manual LCO excitation of the wing was done by hand by pulling the wing mount from below the wind tunnel test section to a minimum angle of 30 degrees.

Another experiment to determine the relationship between LCO amplitude and wind tunnel speed was conducted. In this experiment, conditions were tested with and without a bluff body present. The LCO amplitude was recorded for each interval from 0 to 52.67 Pa in steps of 4.79 Pa.

IV. Results & Discussion

Using manual excitation to find the LCO of the aeroelastic wing, differences were found when the disturbance generator was or was not present. With the disturbance generator stationary, the wing entered LCO beginning at 43.09 Pa. Using fast Fourier transform (FFT) through MATLAB, the LCO frequency was calculated to be 3.43 Hz at a wind tunnel dynamic pressure of 47.88 Pa. LCO without the disturbance generator in the wind tunnel was also found using the same method and dynamic pressure to be 3.41 Hz. When examining the speed at which the wing reaches LCO, starting from 0 Pa, the aeroelastic wing entered LCO when the gust generator was not present from 19.15 Pa to 52.67 Pa. Speeds past 52.67 Pa were not tested. With the gust generator upstream, the aeroelastic wing does not enter LCO at this flow speed and damps out to stationary equilibrium.

When comparing the data from the wing test with and without the disturbance generator in the tunnel, there are several differences to note. With the wind tunnel dynamic pressure at 47.88 Pa, testing with the disturbance generator present found the LCO heave amplitude to have a root mean square (RMS) value of 0.0077 m, as seen in Figure 6. Removing the disturbance generator saw an increase in the RMS amplitude to 0.0097 m, as seen in Figure 7. The same increase in RMS amplitude occurs for pitch angle as well, from 33.64 degrees to 42.87 degrees, as seen in Figures 10 and 11. The FFT plots show that LCO frequencies are roughly equal in both cases. The differences in RMS amplitude of pitch and heave may be caused by the resting disturbance generator still introducing flow disturbances, causing a lower pitch and heave in the wing during LCO.

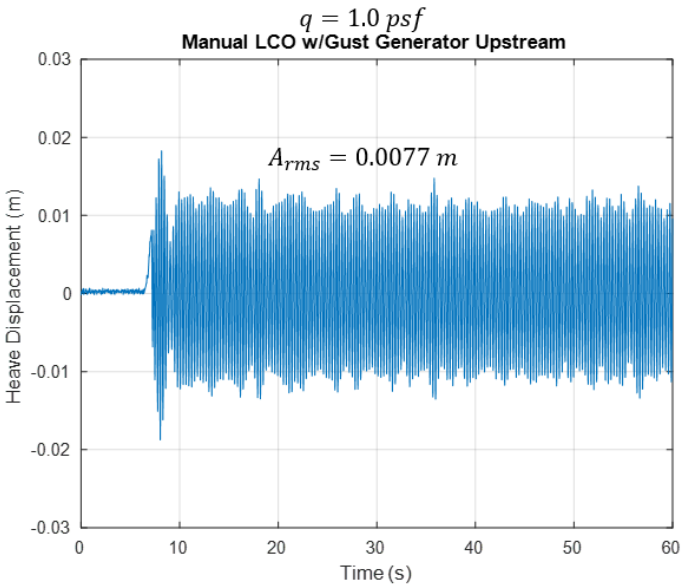

Fig. 6 Heave displacement over time plot of manually displaced aeroelastic wing with gust generator upstream.

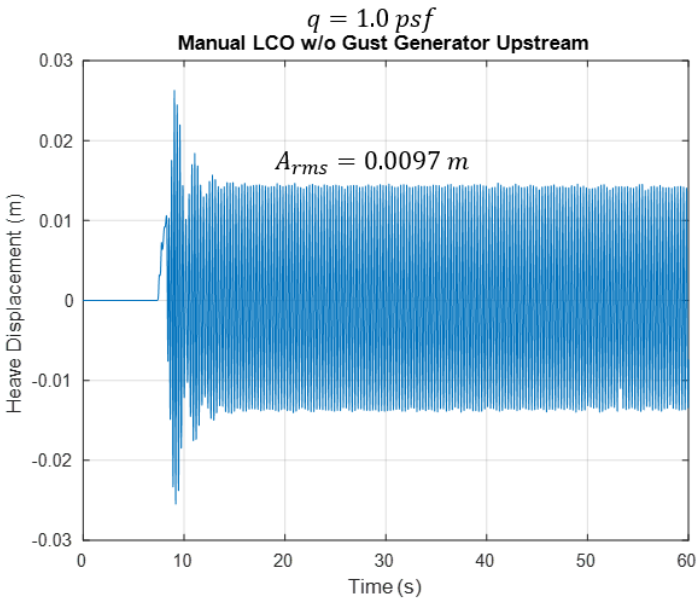

Fig. 7 Heave displacement over time plot of manually displaced aeroelastic wing without gust generator upstream.

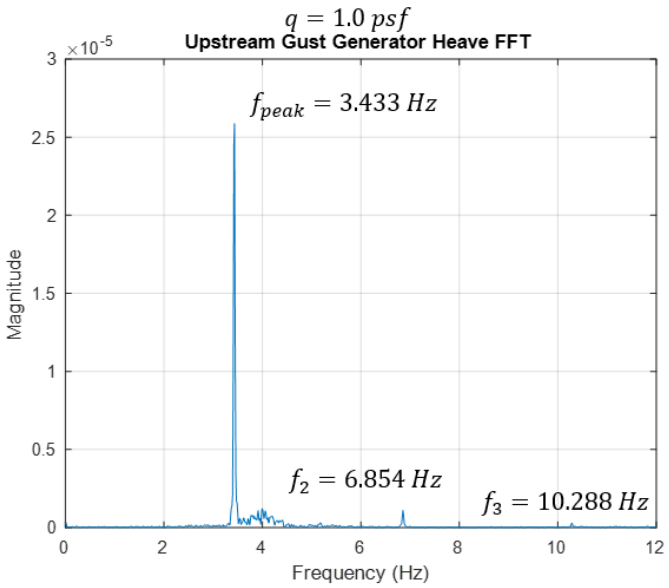

Fig. 8 Fast Fourier Transform (FFT) of heave amplitude with guest generator upstream.

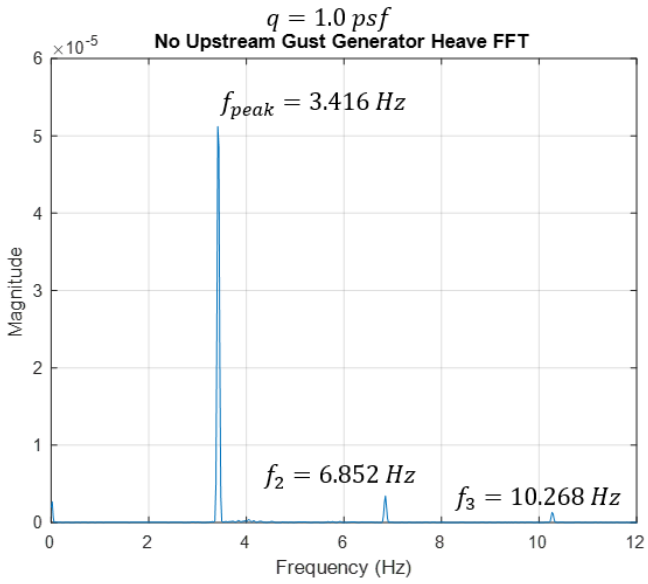

Fig. 9 FFT of heave amplitude without gust generator upstream.

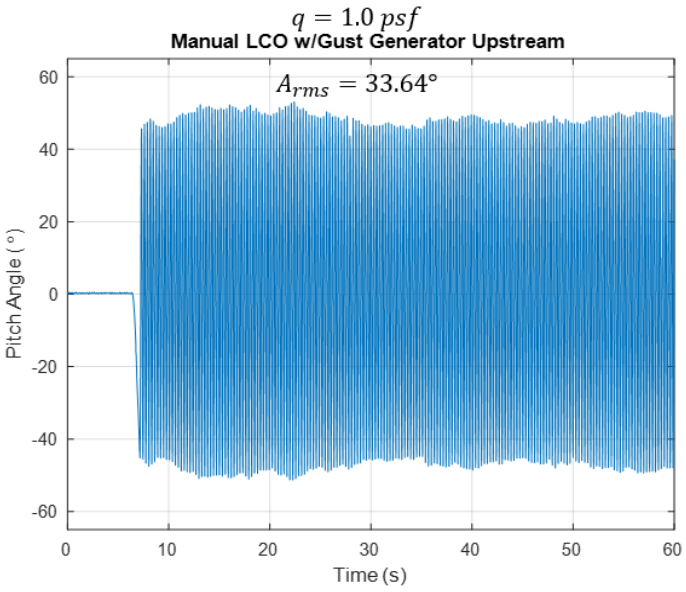

Fig. 10 Pitch angle over time plot of manually displaced aeroelastic wing with gust generator upstream.

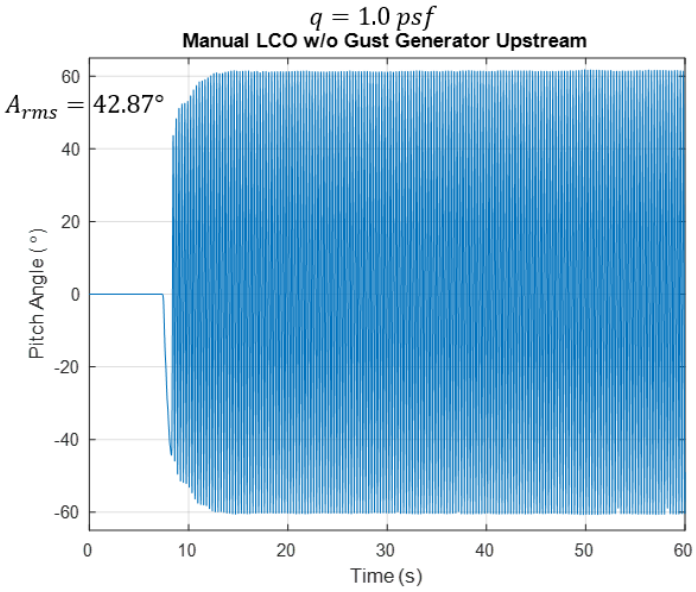

Fig. 11 Pitch angle over time plot of manually displaced aeroelastic wing without gust generator upstream.

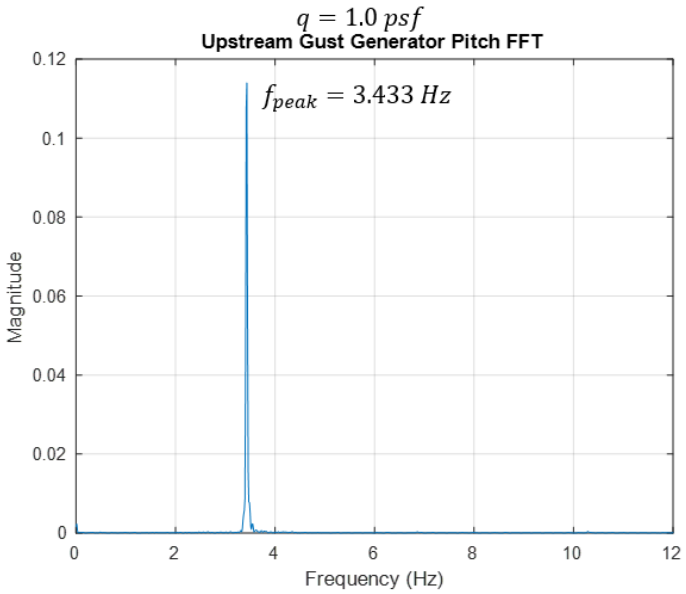

Fig. 12 FFT of pitch angle amplitude with gust generator upstream

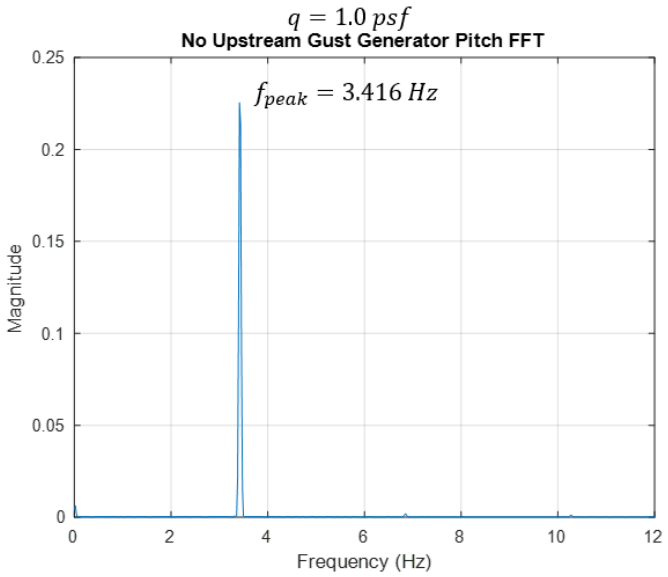

Fig. 13 FFT of pitch angle amplitude without gust generator upstream.

The new aeroelastic wing in comparison with the old wing also serves as another data point when examining changes in mass and its effect on LCO characteristics. At 47.88 Pa, the old wing had a LCO frequency of 4.05 Hz with the disturbance generator upstream, the RMS amplitude of heave was 0.03 m, and the RMS amplitude of pitch was 37.7 degrees. Without the disturbance generator, the LCO frequency was 4.06 Hz, the RMS amplitude of heave was 0.03 m, and the RMS amplitude of pitch was 37.7 degrees. Table 2 below details the differences in LCO characteristics between the old and new aeroelastic wings. Early conclusions from this data show that increasing the total mass while maintaining geometry will decrease the frequency, heave amplitude, and pitch amplitude, all by varying degrees. However, more data is required to draw significant conclusions.

Table 2 Measured differences between old and new aeroelastic wing.

	Property	Old Wing	New Wing
With Disturbance Generator	LCO Frequency	4.05 Hz	3.43 Hz
	RMS Heave	0.03 m	0.0077 m
	RMS Pitch	37.7°	33.64°
Without Disturbance generator	LCO Frequency	4.06 Hz	3.41 Hz
	RMS Heave	0.03 m	0.0097 m
	RMS Pitch	37.7°	42.87°

V. Conclusion

The design update of the aeroelastic wing has been shown to demonstrate self-sustaining LCO in flow speeds as low as 19.15 Pa without upstream disturbances. The increase in mass of the new aeroelastic wing shows a decrease in LCO frequency and RMS pitch and heave amplitude. Further testing of the wing may be done to implement automatic excitation and annihilation of LCO and having a wing of the same geometry, but different mass properties, adds a new data point of comparison for existing studies. The new wing opens possible research into improving characteristics of LCO such as frequency and amplitude, which can be applied to aeroelastic energy harvesting or suppression of aeroelastic instabilities.

Acknowledgments

The author would like to thank Michael Hughes for the set up and data acquisition for wind tunnel testing. The author would also like to thank members of the iSSRL for assistance and guidance in this research.

References

[1] Gianikos, Z. N., Kirschmeier, B. A., Gopalarathnam, A., and Bryant, M., "Limit Cycle Characterization of an Aeroleastic Wing in a Bluff Body Wake," Journal of Fluids and Structures, Vol. 95, 2020, p. 102986.

[2] Kirschmeier, B. A., Gianikos, Z., Gopalarathnam, A., and Bryant, M., "Amplitude Annihilation in Wake-Influenced Aeroelastic Limit-Cycle Oscillations," AIAA Journal, Vol. 58, No. 9, 2020, pp. 4117–4127.

[3] Visbal, M. R., and Garmann, D. J., "Numerical Investigation of Spanwise End Effects on Dynamic Stall of a Pitching NACA 0012 Wing," 2017.

[4] Strganac, Thomas W., et al. "Identification and Control of Limit Cycle Oscillations in Aeroelastic Systems." Journal of Guidance, Control, and Dynamics, vol. 23, no. 6, 2000, pp. 1127–1133.

[5] Goodman, Charles, et al. "An Analysis of the F/A-18C/D Limit Cycle Oscillation Solution." 44th AIAA/ASME/ASCE/AHS/ASC Structures, Structural Dynamics, and Materials Conference, 2003.

[6] Hayes, William Brian and Kelan D. Sisk. "Prevention of External Store Limit Cycle Oscillations on the F/A-18E/F Super Hornet and EA-18G Growler Aircraft." 2008.

[7] Bryant, Matthew, and Ephrahim Garcia. "Development of an Aeroelastic Vibration Power Harvester." SPIE Proceedings, 2009.

[8] Bryant, Matthew, and Ephrahim Garcia. "Energy Harvesting: A Key to Wireless Sensor Nodes." SPIE Proceedings, 2009.

[9] Bryant, Matthew, and Ephrahim Garcia. "Modeling and Testing of a Novel Aeroelastic Flutter Energy Harvester." Journal of Vibration and Acoustics, vol. 133, no. 1, 2011.

[10] Chatterjee, P, and M Bryant. "Aeroelastic-Photovoltaic Ribbons for Integrated Wind and Solar Energy Harvesting." Smart Materials and Structures, vol. 27, no. 8, 2018.